High frequency periodic forcing of the oscillatory catalytic CO oxidation on Pt (110)

2007 New J. Phys. 9 61

(http://iopscience.iop.org/1367-2630/9/3/061)

New Journal of Physics
The open-access journal for physics

High frequency periodic forcing of the oscillatory catalytic CO oxidation on Pt (110)

P S Bodega[1], P Kaira[1], C Beta[2], D Krefting[3], D Bauer[1], B Mirwald-Schulz[1], C Punckt[1] and H H Rotermund[1,4,5]

[1] Fritz-Haber-Institut der Max-Planck-Gesellschaft, Faradayweg 4-6, 14195 Berlin, Germany
[2] Max Planck Institute for Dynamics and Self-Organization, Am Fassberg 11/Turm 2, 37077 Goettingen, Germany
[3] Charité — Universitätsmedizin Berlin, Campus Benjamin Franklin (CBF), Hindenburgdamm 30, 12200 Berlin, Germany
[4] Department of Physics and Atmospheric Science, Dalhousie University, Halifax, NS B3H 3J5 Canada
E-mail: harm.rotermund@dal.ca

New Journal of Physics **9** (2007) 61
Received 11 December 2006
Published 19 March 2007
Online at http://www.njp.org/
doi:10.1088/1367-2630/9/3/061

Abstract. Resonant periodic forcing is applied to catalytic CO oxidation on platinum (110) in the oscillatory regime. The external parameters are chosen such that the unperturbed system spontaneously develops chemical turbulence. By periodically modulating the CO partial pressure, changes in the spatiotemporal behaviour of the system can be induced: the turbulent behaviour is suppressed and frequency locked patterns with sub-harmonic entrainment develop. A novel gas-driving compressor has been implemented to perform the experimental work.

[5] Author to whom any correspondence should be addressed.

PII: S1367-2630(07)39135-0

Contents

1. Introduction

Periodic forcing is ubiquitous in nature. It can be observed in phenomena as diverse as the human heartbeat, circadian rhythm, or tidal currents. Neglecting the spatial degrees of freedom, such systems can be considered as periodically forced nonlinear oscillators. Depending on the amplitude γ and frequency υ_f of the external force, an oscillator may become entrained by the external stimulus, a phenomenon commonly referred to as frequency locking. In the frequency-locked state, the system may oscillate with a frequency υ different from its natural frequency υ_0, where the range of detuning $\upsilon - \upsilon_0$ over which frequency locking can be observed expands for increasing forcing amplitude γ. This is reflected by tongue-shaped regions of resonance in the frequency–amplitude plane. Inside these so-called Arnold tongues, the frequency of the entrained oscillator is rationally related to the frequency of the external force, $\upsilon_f/\upsilon = n/m$, where the general case of an $n : m$ resonance is denoted as sub-harmonic (super-harmonic) if $n > m$ ($n < m$). Periodic forcing and entrainment of single oscillators are well understood and have been investigated in the context of many different systems, see e.g. [1] and references therein.

If a periodic force is applied to an extended system of diffusively coupled oscillators, the situation becomes more intricate. Besides frequency-locked uniform oscillations, complex spatiotemporal phenomena can occur in such systems depending on the choice of frequency and amplitude of the external force. In particular, for an $n : m$ resonance different parts of the system can be locked to any of the n distinct phase states and fronts will be observed that separate these different phase locked states.

Important classes of systems, in which these phenomena can be investigated experimentally, are chemical reaction–diffusion systems with oscillatory kinetics. Previous studies were mostly performed using the periodically forced light-sensitive Belousov–Zhabotinsky (BZ) reaction [2]. Resonant pattern formation in this system has been systematically investigated as a function of the forcing parameters υ_f and γ [3]. A variety of space-time patterns could be stabilized and detailed studies of resonant phase clusters [4] and front instabilities were performed [5].

In recent years, a number of heterogeneous catalytic surface reactions were established as model systems for the study of self-organization in nonlinear reaction–diffusion systems [6]. They belong to a class of chemical reactions with high industrial relevance. Taking place on well-defined single crystal surfaces, these systems are truly two-dimensional and individual

reaction steps can be analysed with surface scientific diagnostics under ultrahigh-vacuum (UHV) conditions. Thus, contrary to homogeneously catalysed reactions in the aqueous phase, their mechanism is often simple and well understood. Among these reactions, the catalytic oxidation of CO on platinum is the most thoroughly studied case [7]. It follows the Langmuir–Hinshelwood mechanism [7]: molecules of CO and O_2 adsorb from the gas phase on the catalytic metal surface (the adsorption of O_2 is dissociative). Adsorbed CO molecules diffuse and react with O to produce CO_2, and subsequently CO_2 desorbs from the surface. An interplay of reaction, lateral diffusion of CO, and adsorbate-induced surface reconstruction (affecting adsorption kinetics of oxygen [8] gives rise to rich spatiotemporal dynamics like homogeneous oscillations, target patterns, spiral waves or chemical turbulence [9]. The dynamics of this reaction can be manipulated by tuning the surface temperature and the partial pressures of the reactants in the gas phase. This approach has been used to control chemical turbulence [10, 11], to engineer spatiotemporal pattern formation by global feedback [12]–[14], and to locally address the surface activity with a focused laser beam [15, 16].

The oscillatory catalytic CO oxidation on platinum can be externally forced by applying periodic variations to the partial pressures of reactants in the chamber. Harmonic resonance of the CO_2 production rate as well as super- and sub-harmonic entrainment were observed for the CO oxidation reaction on Pt(110) under periodic forcing of the oxygen partial pressure and the plane spanned by amplitude and frequency of the external force was systematically mapped [17]. With the development of photoemission electron microscopy (PEEM), the spatially resolved real-time observation of adsorbate patterns on the catalyst surface became possible [18]. This technique was recently employed to image resonant pattern formation under periodic forcing. Starting from spatiotemporally chaotic initial conditions in absence of an external force, intermittent turbulence, disordered cellular structures, labyrinth patterns, and oscillatory phase clusters could be stabilized by periodic modulation of the CO partial pressure in the reactor [12].

Theoretical work mostly focused on the forced complex Ginzburg–Landau equation (CGLE), a generic model for oscillatory reaction–diffusion system close to a supercritical Hopf bifurcation [19]. In this model, the dynamical properties and instabilities of fronts between different phase-locked domains were investigated in detail [20]–[24]. Moreover, the effect of diffusion on frequency locking has been studied [25] together with synchronization scenarios [26] and the emergence of stripe patterns [27].

In a recent theoretical contribution, Davidsen *et al* [28] studied the dynamics of fronts between phase-locked domains in resonantly forced catalytic CO oxidation on Pt(110). Their numerical investigations were carried out using the Krischer–Eiswirth–Ertl (KEE) model, a well-established realistic model of the CO oxidation reaction [29]. Motivated by similar observations in the forced CGLE [30, 31], they focused on explosion-type front instabilities that can be observed if the forcing amplitude is decreased below a critical value. In the 2 : 1 resonantly forced regime, this instability gave rise to a disordered state of defect mediated turbulence, whereas a labyrinthine structure emerged in the case of 3 : 1 resonance. Depending on the detuning $(\upsilon_f - \upsilon_0)$, a cascade of period doubling bifurcations was observed as the front instability was approached with decreasing forcing amplitude. Interestingly, in the case of 3 : 1 resonance, a bistability between 3 : 1 and 2 : 1 locking to the external force can be observed.

Previous experimental efforts to study pattern formation in catalytic CO oxidation under external periodic forcing were restricted to forcing frequencies not larger than twice the natural frequency of the system. The amplitude of partial pressure modulation in the reactor was limited by the finite pumping speed of the vacuum chamber [12]. In the present study, we introduce

a new experimental set-up that allows for the first time to impose higher forcing frequencies to the CO oxidation reaction, while at the same time spatiotemporal concentration patterns on the catalyst surface can be imaged by PEEM. After a detailed description of the apparatus, we employ the improved set-up to test some of the recent predictions by Davidson *et al* [28]. A sufficiently large forcing amplitude γ results in suppression of chemical turbulence and leads to phase locked regimes where cluster patterns or homogeneous oscillations occur.

2. Experimental set-up

We present experiments on catalytic CO oxidation that are performed on a platinum (110) single crystal sample in an UHV-chamber. The chamber is connected to a gas-dosing system and equipped with standard surface diagnostic instruments (mass-spectrometer, low energy electron diffraction (LEED), Auger electron spectroscopy (AES), ionization manometer, absolute pressure gauge). The set-up allows controlling the sample temperature and the partial pressures of the reaction educts either manually or computer controlled using LabView (National Instruments Corporation). Adsorbate coverages are imaged via changes in the local work function using a PEEM. The resulting images are recorded by a Sony CCD camera, while the experimental parameters and the mean intensity of a 10×10 pixel region of the PEEM image are stored by a computer with a sampling rate of 10 Hz.

All experiments are performed within the following parameter range: temperature 512–529 K, oxygen partial pressure $1.0–1.5 \times 10^{-4}$ mbar, carbon monoxide base pressure $7.2–9.3 \times 10^{-5}$ mbar. Under these conditions, the chemical reaction–diffusion system shows oscillatory behaviour with a natural frequency in the range of $\upsilon_0 \approx 1$ Hz (see results and discussion, section 3.1).

For resonant forcing, the carbon monoxide pressure p_{co} in the chamber is periodically modulated according to

$$p_{\mathrm{co}}(t) = p_{\mathrm{co}_0}[1+\gamma \ \sin\ (2\pi \cdot \upsilon_{\mathrm{f}} \cdot t)],$$

with γ indicating the forcing amplitude and $\nu_{\mathrm{f}} \approx n\nu_0 (n \epsilon \mathrm{IN})$ the forcing frequency. T and p_{oxygen} are held constant during the experiment.

The general procedure for all experiments is as follows.

1. Preparation of the sample by Ar-ion sputtering and subsequent annealing at 950 K.
2. Rough manual adjustment of T, p_{oxygen} and p_{co} to reach the system's oscillatory regime, monitored with PEEM.
3. Manual fine tuning of the parameters until the uniform oscillations become spatially unstable and show turbulent behaviour.
4. Measurement of the system's natural frequency (see results and discussion, section 3.1).
5. Application of harmonic modulation of p_{co} and measurement of the system response using the PEEM images.

For forcing frequencies $\upsilon_{\mathrm{f}} \leqslant 2$ Hz, we use an electronic valve to control the carbon monoxide flux. The valve is connected to a computer and is regulated by an oscillating voltage

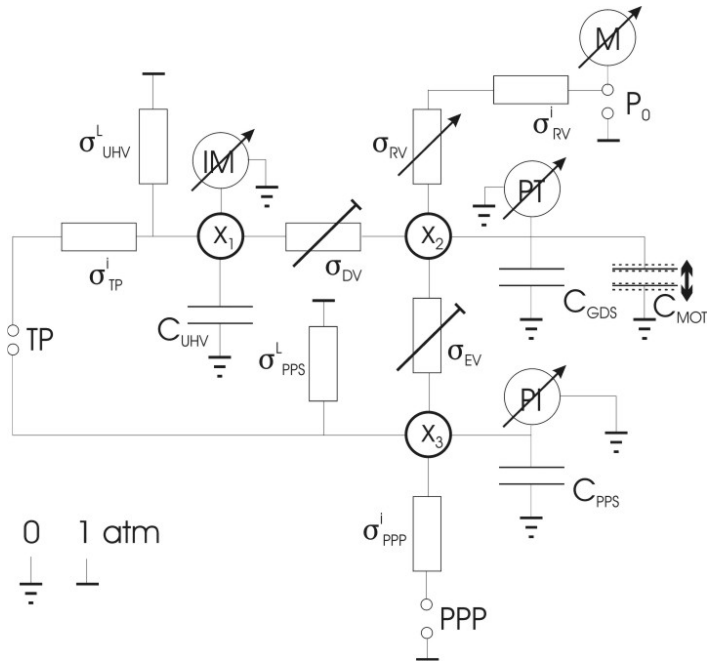

Figure 1. The CO pressure regulating system represented as an electric circuit. Symbols, abbreviations and indices: σ = conductivity, C = capacity, x_1 = pressure in UHV-chamber, x_2 = regulated CO pressure in gas dosing system, x_3 = pressure in prepressure system, DV = dosing valve, EV = exhaust valve, GDS = gas dosing system, i = inner, IM = ionization manometer, L = leakage, M = manometer, MOT = compressor, P_0 = pressure after manometer, PPP = prepressure pump, PPS = prepressure system, PI = Pirani pressure sensor, PT = pressure transducer, RV = regulating valve, TP = turbo pump, UHV = ultra high vacuum.

signal generated by LabView. This set-up provides the ability to scan over a predefined range of forcing amplitudes and frequencies to measure the system's response in a wide range of parameter space.

However, this set-up fails for higher forcing frequencies, as the forcing amplitude is strongly damped. Based on the analogy between electrical and pneumatic circuits [32] the UHV-chamber and the CO pressure regulating system were analysed in detail. Even if this analogy neglects chemical forces and the finite velocity of the gas stream, it reveals the intrinsic low pass filtering characteristics of the system as can be deduced from the equivalent circuit diagram (figure 1).

To overcome these experimental restrictions, a novel gas-regulating device was developed and implemented into the system to substitute the electronic valve. The heart of the new device is a simple plunger, connected to the CO prepressure line with a branch connection (see figure 2). By periodically moving the main piston in and out of its cylinder with the help of a stepper motor, the gas line volume is changed accordingly, resulting in a harmonic modulation of the CO pressure. The amplitude depends on the ratio between the plunger volume and the installed gas line volume and can be regulated in a wide range by utilizing a secondary cylinder as an offset

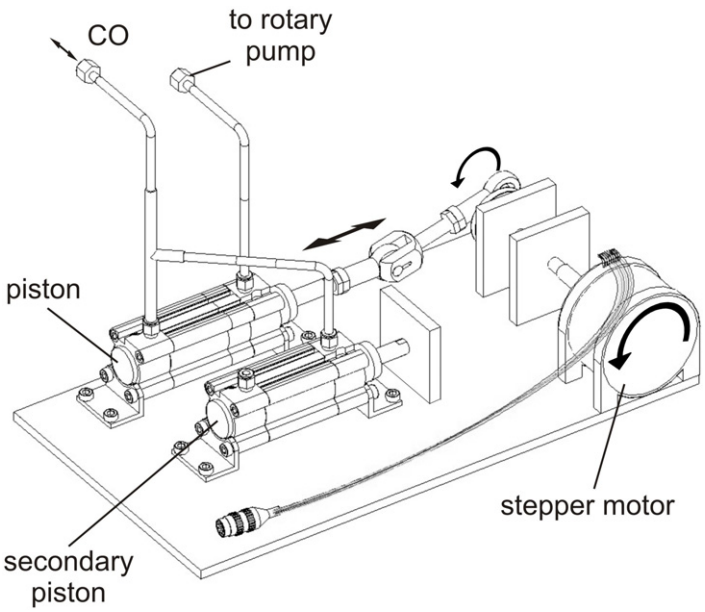

Figure 2. Design of the forcing compressor.

gas volume within the prepressure system. The forcing frequency is adjusted by the rotational frequency of the stepper motor driving the piston compressor. The other side of the piston is pumped by a rotary pump to ease the movement of the piston, since the CO pressure is normally operated between 50 and 100 mbar.

This new device allows us to apply periodic forcing at frequencies up to 4 Hz and well-defined amplitudes. We have analysed the frequency response inside the UHV-chamber to the generated pressure changes in the prepressure line and present the results in the form of a Bode plot in figure 3. The measurement was performed at $p_{\mathrm{co}} = 2 \times 10^{-4}$ mbar using an ionization manometer (Leybold IM510 with VIG17-head) in linear scaling. The oscillation amplitude in the gas dosing system was around 20%. We estimated that at a frequency of 2 Hz the effective pressure variation in the UHV-chamber was 10%. This high value could only be achieved under optimal forcing conditions; under not so favourable conditions, the forcing strength is reduced by about one order of magnitude.

3. Results and discussion

3.1. The natural frequency of the system

Uniform oscillations in a spatially extended system can become unstable resulting in chaotic patterns, where the underlying local dynamic is still oscillatory. This behaviour, characterized by irregular and spatiotemporal disordered patterns, is referred to as chemical turbulence. An analysis of such turbulences can be done through the statistical properties of topological defects in the system [33]. In contrast to chaotic oscillators, the local oscillations in our system are mainly periodic, disturbed only by the diffusive coupling between neighbouring surface sites. The transition from homogeneous oscillations with a defined natural frequency to turbulence is smooth and results in a broadening and small shift of the dominating frequency line. We define

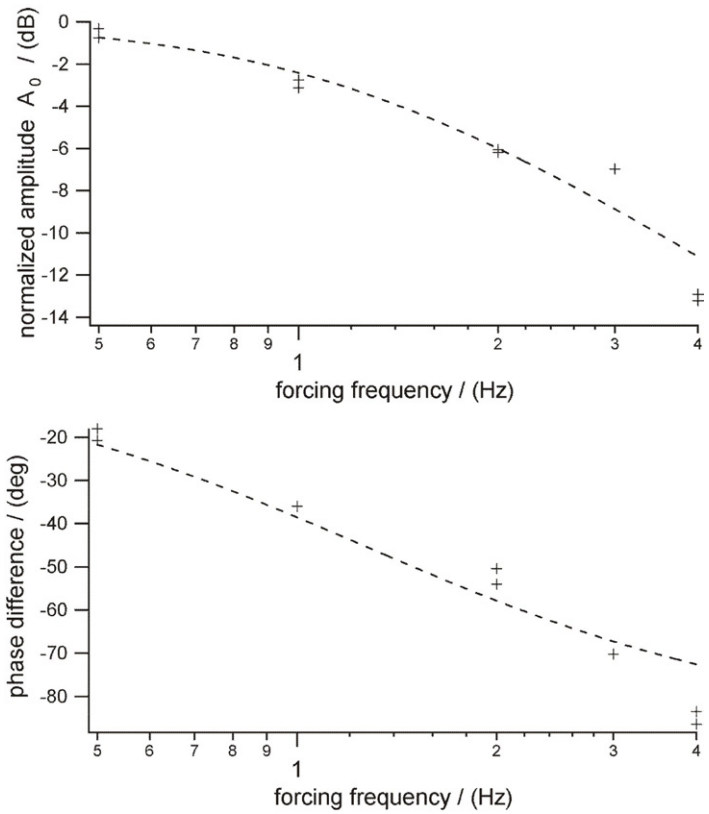

Figure 3. Characteristic Bode-plots of the UHV-chamber showing the compressor forcing frequency versus phase and amplitude of resulting oscillations inside the UHV-chamber. The experimental results are shown as crosses, while the dashed lines indicate the approximation fits with a first order low pass filter function.

the natural frequency of our system (υ_0) as the main frequency in the Fourier spectrum of the local PEEM intensity, i.e., the frequency with the highest amplitude in the power spectrum of a local intensity time series.

For a measurement of the natural frequency during the experiments, a section of the PEEM image with a size of 10 × 10 pixels is chosen, its mean intensity is calculated, and its time series Fourier transformed (figure 4). From the maximum in the power spectrum the natural frequency is determined.

Even though the frequency analysis is performed locally, its validity is assumed for the whole sample. To prove this assumption, 2500 pixels, equally distributed over the region of interest (figure 5), were chosen from the same video sequence. The time series of one single pixel is shown in figure 6. For each pixel, a fast Fourier transform (FFT) of the time series was computed. Figure 6 shows the result for a random pixel. Although the data are much noisier than in the spatially averaged analysis, the main frequency is the same as in figure 4.

The system frequency mainly depends on the crystal temperature and the partial pressures of the reaction educts. However, on a timescale of several minutes the natural frequency slowly decreases although the reaction parameters are kept constant (figure 7). This effect is presumably caused by a faceting of the platinum surface, which is known to take place at the reaction

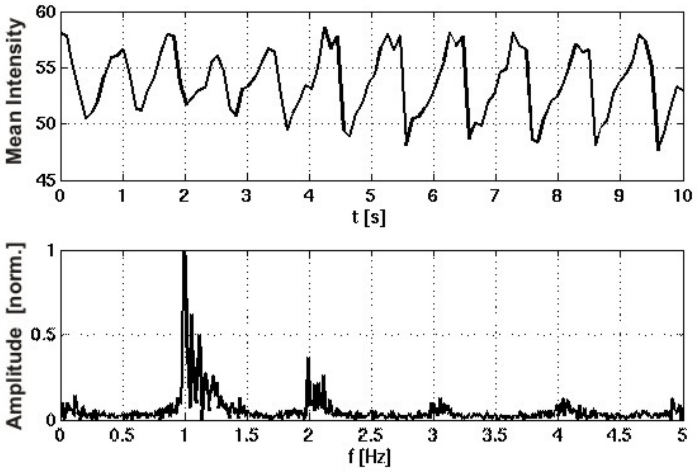

Figure 4. Time series of the averaged image intensity in an area of 10×10 pixels (top panel) and power spectrum of the data (bottom panel). The 1 Hz oscillations are clearly seen in both the time series and the spectrum. The reaction parameters are $T = 515\,\mathrm{K}$, $p_{\mathrm{oxygen}} = 1.5 \times 10^{-4}$ mbar, base $p_{\mathrm{co}} = 7.5 \times 10^{-5}$ mbar.

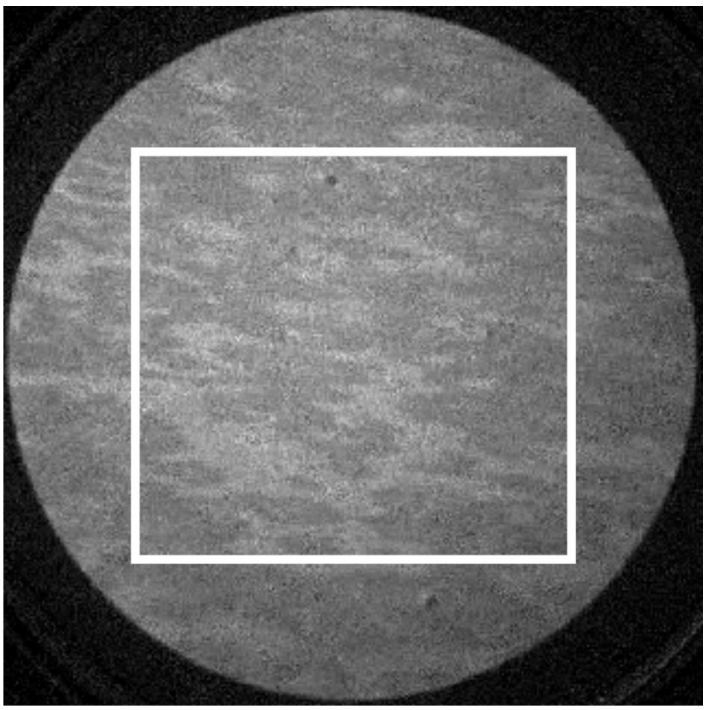

Figure 5. PEEM image of the Pt(110) surface under reaction conditions without forcing. The region of interest (ROI), which was used for a global test of the Fourier method for determination of the natural frequency is indicated by the square. Within the ROI 50×50 pixels were analysed. The reaction parameters are $T = 515\,\mathrm{K}$, $p_{\mathrm{oxygen}} = 1.5 \times 10^{-4}$ mbar, base $p_{\mathrm{co}} = 7.5 \times 10^{-5}$ mbar.

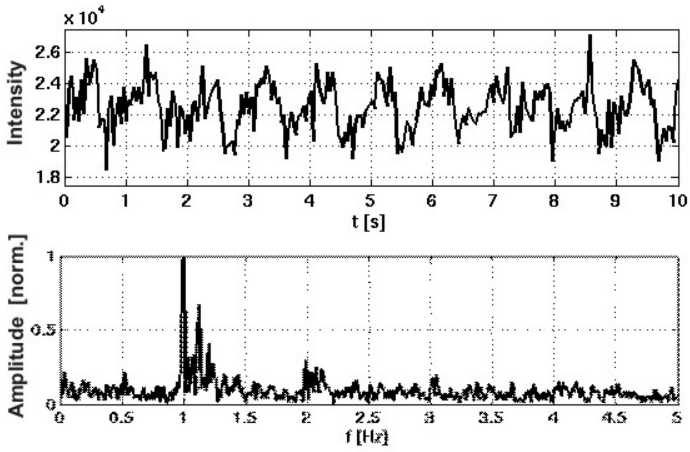

Figure 6. Time series of the grey value of one single pixel (top panel) and respective power spectrum (bottom panel). The reaction parameters are $T = 515\,\mathrm{K}$, $p_{\mathrm{oxygen}} = 1.5 \times 10^{-4}\,\mathrm{mbar}$, base $p_{\mathrm{co}} = 7.5 \times 10^{-5}\,\mathrm{mbar}$.

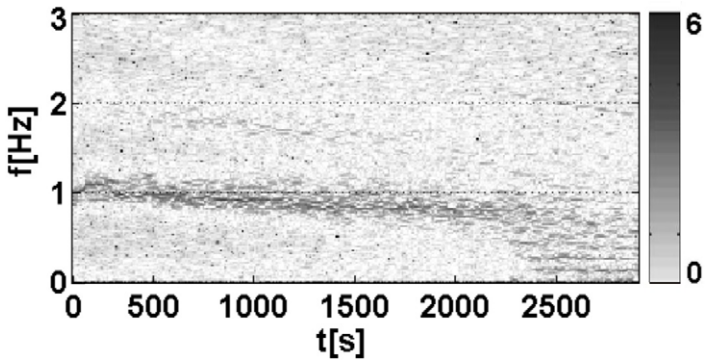

Figure 7. Fourier spectrogram showing the time evolution of the natural frequency of the system without forcing. For each time moment an interval of 20.48 s (512 samples at 25 frames per second) is analysed. Initially the frequency has a value of about 1 Hz. During the first 30 min it drops approximately 0.2 Hz. Also a broadening of the frequency line is observed which indicates, that the system has developed into a more turbulent state. Values of temperature ($T = 515\,\mathrm{K}$), and partial pressures ($p_{\mathrm{oxygen}} = 1.1 \times 10^{-4}\,\mathrm{mbar}$, $p_{\mathrm{co}} = 9.07 \times 10^{-5}\,\mathrm{mbar}$) were constant.

conditions used [34]. This assumption is supported by LEED pictures taken before and after each experiment, showing a broadening of the diffraction spots after the experiment (data not shown).

3.2. 2 : 1-Forcing: entrainment and cluster formation

We apply resonant forcing to our system (υ_{f} close to $2\upsilon_0$). For sufficiently large forcing amplitudes this results in an entrained state, where the oscillation frequencies of the system and the forcing signal maintain a fixed ratio $m : n$ (m and n natural numbers). Starting with a turbulent system state, forcing frequencies closely above $2\upsilon_0$ were scanned, while applying

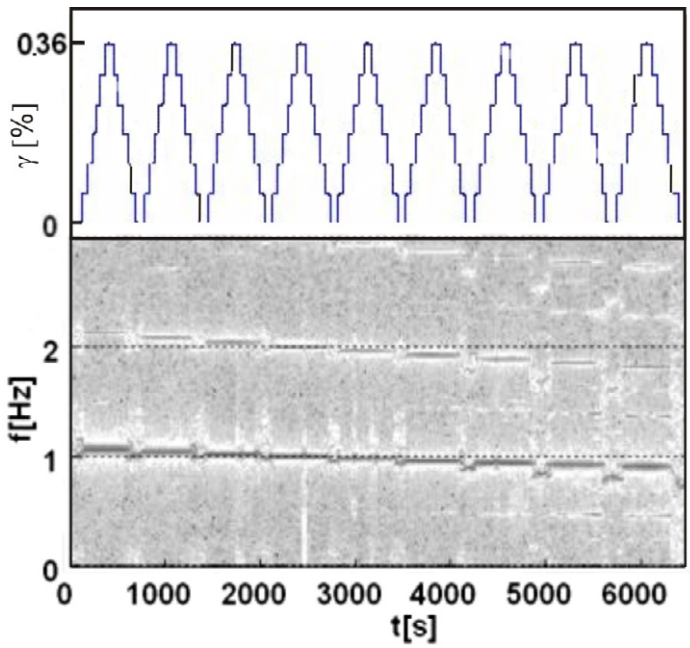

Figure 8. Fourier spectrogram showing 2 : 1 forcing with 2 : 1 entrainment for sufficiently high forcing amplitudes. Top panel: forcing amplitude as a function of time. Bottom panel: corresponding Fourier spectra from 20.48 s intervals. The forcing amplitude is increased in six steps to 0.36% of the CO base pressure and then decreased to zero again. In each of these amplitude sweeps another forcing frequency is used. The first sweep ($t = 0$–750 s). The last sweep proceeds at 1.92 Hz. During the experiment the natural frequency decreases from around 1–0.8 Hz. The reaction parameters are $T = 512$ K, $p_{\text{oxygen}} = 1.5 \times 10^{-4}$ mbar, base $p_{\text{co}} = 7.2 \times 10^{-5}$ mbar and $\upsilon_0 \sim 1$ Hz.

different γ values between 0 and 0.36% (figure 8). The corresponding frequency analysis reveals that for low frequency mismatch (detuning $\upsilon_{\text{f}}/2 - \upsilon_0$) $\gamma = 0.06\%$ is sufficient to entrain the system, while at larger frequency mismatch entrainment occurred only above $\gamma = 0.18\%$. In the measurement shown in figure 8, the system is 2 : 1 entrained, since it oscillates predominantly at a frequency close to half of the frequency of the external force, $\upsilon_{\text{f}}/2$. At higher mismatch, a period doubling occurs as can be seen from the appearance of sub-harmonic frequencies around $t = 5000$ s. This is in agreement with theoretical results obtained by Davidsen *et al* [28] who also found a period doubling scenario in the corresponding Arnold tongue (figure 9).

In a second experiment, we manually adjusted the forcing frequency to $2\upsilon_0$. At this setting a forcing strength of 0.04% was sufficient to suppress turbulent dynamics, at least temporarily. Intermittent turbulent regimes alternated with spatially coordinated patterns. An increase of the forcing strength resulted in shorter turbulent regimes. At $\gamma = 0.22\%$. a phase locked regime with stable cluster patterns, 2 : 1 entrained, was observed (figure 10); the surface splits into large domains belonging to either of the two different phase-locked states. The arising spatiotemporal patterns exhibit a periodicity of four forcing cycles, which indicates that the system performs period doubled 2 : 1 entrained oscillations. Due to the non-harmonicity of the CO oxidation, the size of these phase domains is not fixed but changes in time undergoing enlargement–reduction (breathing like) cycles with a periodicity that is again four times the forcing cycle.

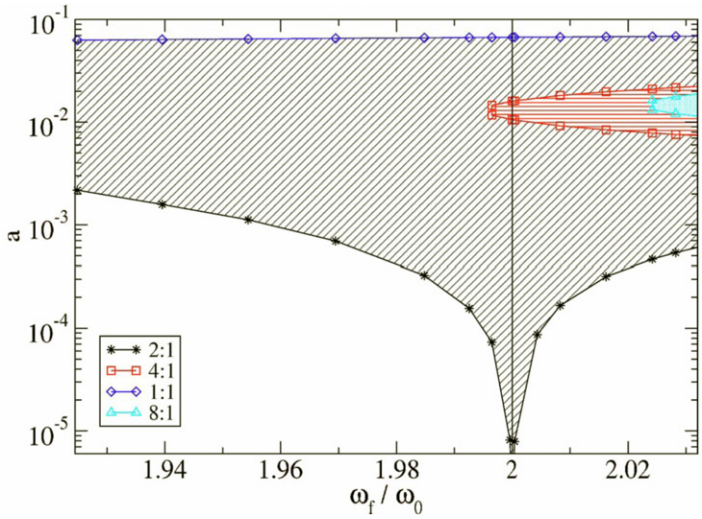

Figure 9. The 2 : 1 Arnolds tongue obtained from numerical simulations with the KEE model [29]. The amplitude of the forced oscillation is plotted as a function of the forcing frequency (normalized to the natural frequency of the system). A period-doubling cascade appears within the tongue in a region below the overlapping 1 : 1 tongue. For $\upsilon_f/\upsilon_0 = 2$ only the first period doubling bifurcation is present. Its location matches with the observed location for a spatially extended system. Reproduced from [28].

The temporal dynamics of each individual image pixel can be separated into phase and amplitude dynamics using a frequency demodulation technique. This is done by Fourier transformation and evaluation of the complex Fourier coefficients at $\upsilon_f/2$ within shifted time intervals of 5 s duration. In polar coordinates these Fourier coefficients directly give phase and amplitude of the dominant mode of the local oscillations. The image pixels can now be coloured corresponding to their respective phase and amplitude. The result is shown in figures 11(a) and (b). Two different surface regions with opposite phase but identical amplitude can clearly be distinguished. A phase portrait of the system is obtained by plotting the phase and amplitude values of all image pixels in polar coordinates (figure 11(c)). In addition, a phase histogram was calculated (figure 11(d)). Two different clusters with a phase difference of π can be seen, while the link between them, corresponding to the bordering area where the oscillations have smaller amplitude, is close to the origin in the phase portrait.

The existence of two stable entrained states differing by a phase shift of π is a property of the 2 : 1 resonance, distinguishing it from the 1 : 1 resonance regime [35]. We observe non-equilibrium Bloch walls as the borders between two different entrained states (π-fronts). They show travelling behaviour and annihilate each other upon collision (figure 12). Their propagation speed has a constant value of $0.35\,\mu\mathrm{m\ s^{-1}}$.

Comparable phase clusters were already found by Bertram *et al* [12] in the case of resonant low frequency forcing with high amplitude. Our results are obtained at 2 : 1 resonant frequency (1.4 Hz instead of 0.67 Hz), with forcing amplitudes more than one order of magnitude smaller.

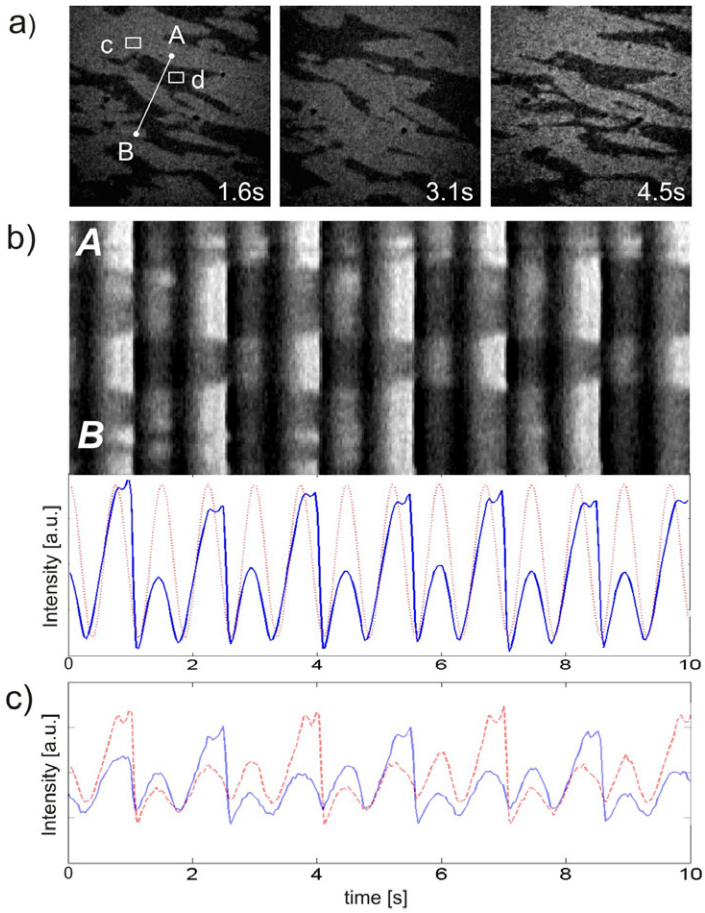

Figure 10. Oscillating clusters during the 2 : 1 forcing experiment. (a) Snapshots of PEEM images 300 × 300 μm^2 illustrating a phase locked regime. (b) Space-time plot taken along the *AB* line (top panel), and the corresponding intensity of the PEEM image (bottom panel) averaged globally (continuous blue line) and the forcing signal (dotted red line). (c) Local values of the intensity, calculated over rectangles *c* (dotted red line) and *d* (continuous blue line). The reaction parameters are $T = 529\,\mathrm{K}$, $p_{\mathrm{oxygen}} = 1 \times 10^{-4}\,\mathrm{mbar}$, base $p_{\mathrm{co}} = 9.26 \times 10^{-5}\,\mathrm{mbar}$, γ is 0.22% of the CO pressure base value. $\upsilon_0 = 0.7\,\mathrm{Hz}$, and $\upsilon_{\mathrm{f}} = 1.4\,\mathrm{Hz}$.

3.3. 3 : 1-Forcing

Analogous experiments were carried out driving the system with three times its natural frequency ($\upsilon_{\mathrm{f}} = 3\upsilon_0$). At a forcing strength of about 0.12%, phase locked regimes were observed (figure 13). As can be seen in the *xt*-plot (figure 13(b)), the system largely performs oscillations with a frequency of $\upsilon = \upsilon_{\mathrm{f}}/2$ (2 : 1 entrainment). An analysis of the local oscillations (figure 13(c)) reveals that—like in the case of 2 : 1 forcing—an additional shoulder appears during every oscillation cycle. However, it seems that for this amplitude of 3 : 1 forcing the system is not fully entrained. At $t = 5.5\,\mathrm{s}$ the pattern inverts: in the *xt*-plot a large amplitude oscillation is not followed by a small shoulder but by another large amplitude oscillation. After this transition, the oscillations of the system are again 2 : 1 entrained. These more complex dynamics are also visible

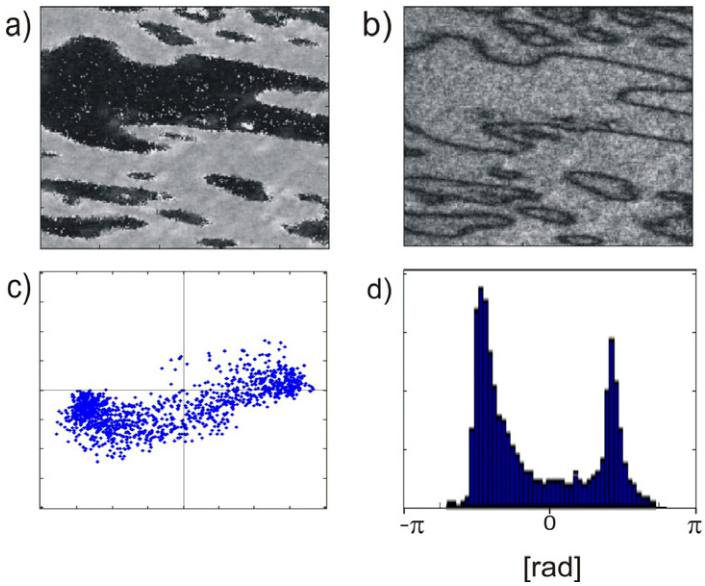

Figure 11. Phase and amplitude representation of the cluster patterns shown in figure 10. (a) Phase pattern, (b) amplitude pattern, (c) phase portrait and (d) phase histogram.

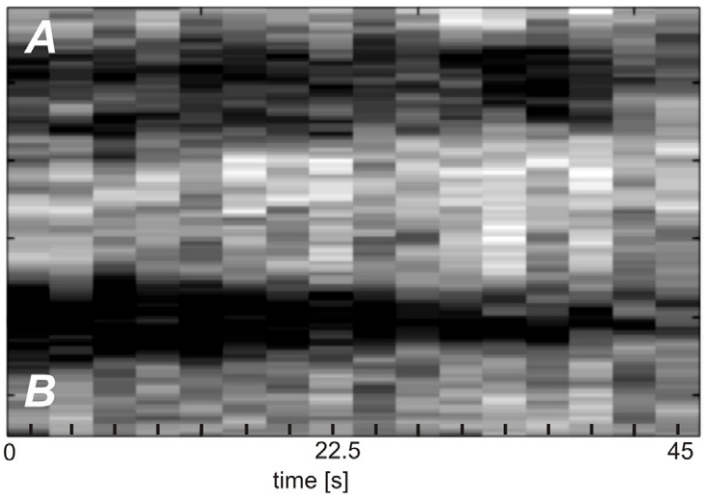

Figure 12. Space-time stroboscopic plot showing the pattern evolution along the same *AB* line of figure 10, choosing one frame every four forcing cycles (2.84 s). Four Bloch walls separating different phase locked domains are identified; two of them approach to each other at a constant speed of 0.35 μm s^{-1}.

when phase and amplitude of the patterns are analysed (figure 14). Two distinct clusters with sharp boundaries can be observed (figures 14(a) and (b)). In contrast to 2 : 1 forcing, they have different amplitude and are not separated by a phase difference of π (figure 14(c)). Moreover, the temporal evolution of the phase histogram (figure 14(d)) shows that the phase difference between the two clusters changes in the course of time (video clip 1 and 2). The two domains approach each other in phase space until a part of the cluster that lags behind skips half an oscillation cycle.

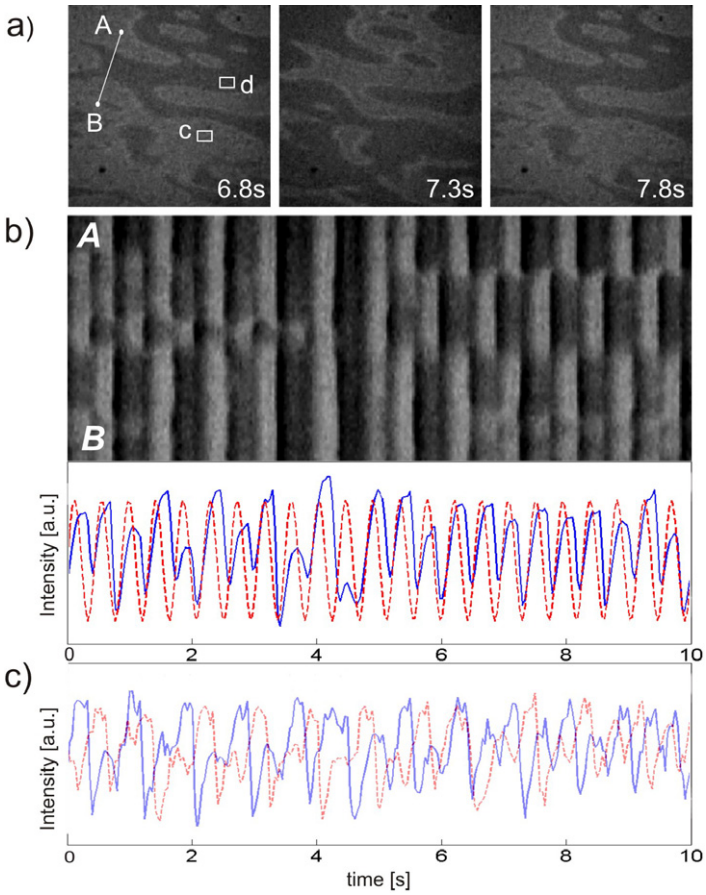

Figure 13. Oscillating clusters during the 3 : 1 forcing experiment with 2 : 1 entrainment. (a) Snapshots of PEEM images (size $300 \times 300\,\mu\text{m}^2$). (b) Space-time plots showing the pattern evolution along the AB line (top panel), and corresponding greyscale values of the PEEM image (continuous blue line) averaged over the whole snapshot, and the applied forcing signal (dotted red line). (c) Local values of the intensity, calculated over rectangles c (continuous blue line) and d (dotted red line). The reaction parameters are $T = 526\,\text{K}$, $p_{\text{oxygen}} = 1.5 \times 10^{-4}\,\text{mbar}$, base $p_{\text{co}} = 6.9 \times 10^{-5}\,\text{mbar}$, γ is 0.12% of the CO pressure base value, $\upsilon_0 = 0.76\,\text{Hz}$ and $\upsilon_{\text{f}} = 2.3\,\text{Hz}$.

This is visible as the transfer of a shoulder from one peak to the other in the phase histogram and coincides with the inversion of the oscillation pattern in the xt-plot. After this inter-cluster transfer, the phase difference has a value of π but subsequently starts to shrink again. The more complex behaviour of the system is probably caused by the competition between the natural frequency υ_0 and the enforced actual oscillation frequency which has a ratio of 2 : 3.

As in subsection 3.2, the non-harmonicity of the CO oxidation plays a role in the size of the clusters formed, which undergo periodic changes ('breathing' every two forcing cycles), though less pronounced in this case.

The cluster boundaries behave similar to the Bloch walls observed in 2 : 1 forcing. They are characterized by a minimum in the oscillation amplitude and move slowly (figure 15).

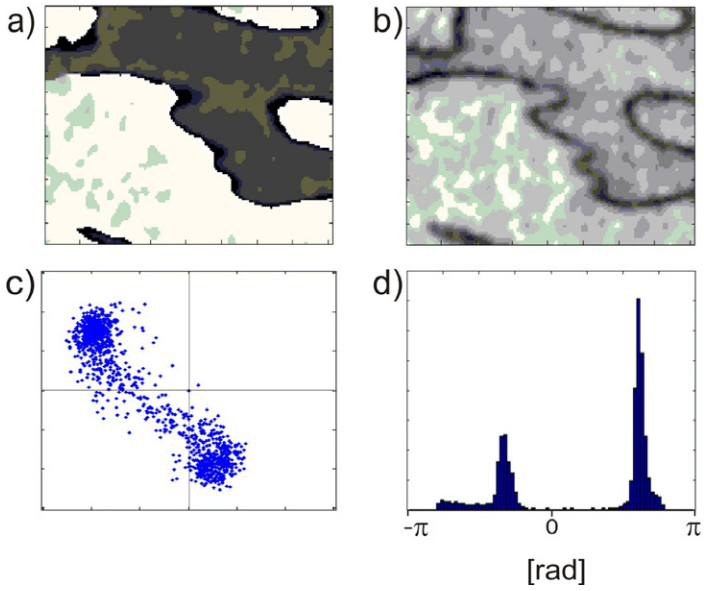

Figure 14. Phase and amplitude representation of the cluster patterns shown in figure 13. (a) Phase pattern, (b) amplitude pattern, (c) phase portrait and (d) phase histogram.

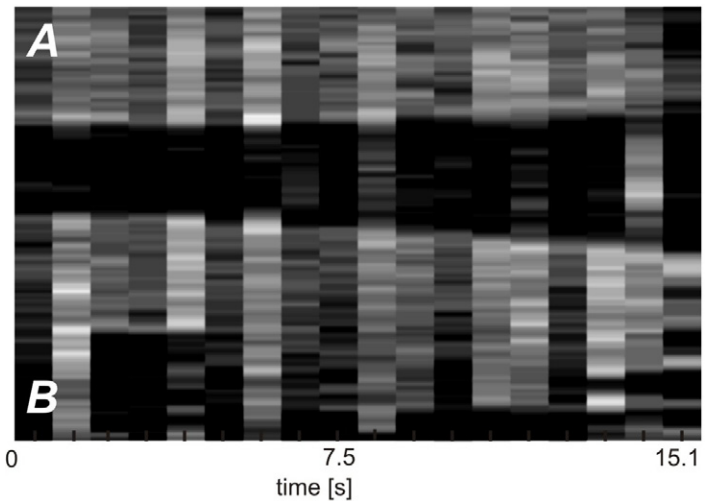

Figure 15. Space-time stroboscopic plot showing the pattern evolution along the same *AB* line of figure 13, but choosing one frame every two forcing cycles (0.84 s). Cluster boundaries separating different phase locked domains move apart.

4. Conclusions

In order to study the effects of periodic external forcing on chemical turbulence in CO oxidation on Pt(110), we designed and built a compressor driven reactor which allows global gas phase forcing for frequency modulations up to 4 Hz. Experiments in two different resonant forcing regimes were

performed (namely 2 : 1 and 3 : 1) and the observed pattern formation is discussed with respect to experimental and previous theoretical studies. For particular values of the amplitude under 2 : 1 and 3 : 1 forcing, the system evolved to a regime dominated by phase locked cluster-domains.

The variety of patterns observed in the 2 : 1 forcing experiments is enlarged by a period doubling scenario. This dynamics turned out to be more complex for the 3 : 1 case: the intuitive distribution into three phase locked domains is replaced by the dynamically changing pattern of two domains and a transfer shoulder affecting the phase difference. This may be caused by the asymmetrical ratio of the 3 : 1 resonant forcing and the observed 2 : 1 entrainment, within the frame of the anharmonic chemical oscillations.

Phase fronts separating different homogeneous phase locked states are clearly observed during our experiments. In addition, theoretical work [28] predicts front explosions for decaying forcing amplitudes: turbulent interfacial zones for 2 : 1 resonant forcing and labyrinth patterns for the 3 : 1 case. This could not be observed in our experiments, probably due to the high sensitivity of the system to parameter changes and present technical limitations in the application of soft changes in γ. Every parameter change in our set-up is followed by a short period of self-adjustment of the system, long enough to perturb the reaction dynamics significantly, and thus transition dynamics between different patterns cannot be resolved.

The corresponding Bloch walls in our system travel with a certain velocity and direction. According to theoretical predictions, they may undergo oscillatory movements if particular conditions are fulfilled (for instance, in the Benjamin–Feir unstable regime). These changes in the cluster dynamics occur on the timescale of minutes. During our experiments, however, the crystal undergoes slow structural changes due to surface faceting, affecting the stability of the entrained states (see subsection 3.1). This strongly limits the precise characterization of the behaviour of the π-fronts, which requires recording over a larger number of oscillation cycles.

In summary, we described a new compressor to induce a variety of spatiotemporal patterns in experiments of forced catalytic CO oxidation on Pt(110) reaching, for the first time, the 3 : 1 forced regime. Our findings agree with the results of numerical simulations of the forced KEE model of catalytic CO oxidation.

Acknowledgments

Financial support of the Marie Curie European ‘Patterns’ project, and the SBF 555 ‘Complex Nonlinear Processes’ are gratefully acknowledged. We thank A S Mikhailov, O Rudzick and M Eiswirth for helpful discussions.

References

[1] Pikovsky A, Rosenblum M and Kurths J 2001 *Synchronization: A Universal Concept in Nonlinear Science* (Cambridge: Cambridge University Press)

[2] Petrov V, Ouyang Q and Swinney H L 1997 Resonant pattern formation in a chemical system *Nature* **388** 655–7

[3] Lin A L, Hagberg A, Ardelea A, Bertram M, Swinney H L and Meron E 2000 Four-phase patterns in forced oscillatory systems *Phys. Rev. E* **62** 3790–8

[4] Vanag V K, Zhabotinsky A M and Epstein I R 2001 Oscillatory clusters in the periodically illuminated, spatially extended Belousov–Zhabotinsky reaction *Phys. Rev. Lett.* **86** 552–5

[5] Marts B, Martinez K and Lin A L 2004 Front dynamics in an oscillatory bistable Belousov–Zhabotinsky chemical reaction *Phys. Rev. E* **70** 056223
[6] Imbihl R and Ertl G 1995 Oscillatory kinetics in heterogeneous catalysis *Chem. Rev.* **95** 697–733
[7] Engel T and Ertl and G 1979 Elementary steps in the catalytic oxidation of carbon monoxide on platinum metals *Adv. Catal.* **28** 1
[8] Gritsch T, Coulman D, Behm R J and Ertl G 1989 Mechanism of the CO-induced 1×2–1×1 structural transformation of Pt(110) *Phys. Rev. Lett.* **63** 1086–9
[9] Jakubith S, Rotermund H H, Engel W, von Oertzen A and Ertl G 1990 Spatiotemporal concentration patterns in a surface-reaction: propagating and standing waves, rotating spirals, and turbulence *Phys. Rev. Lett.* **65** 3013–6
[10] Kim M *et al* 2001 Controlling chemical turbulence by global delayed feedback: pattern formation in catalytic CO oxidation on Pt(110) *Science* **292** 1357–60
[11] Beta C, Bertram M, Mikhailov A S, Rotermund H H and Ertl G 2003 Controlling turbulence in a surface chemical reaction by time-delay autosynchronization *Phys. Rev. E* **67** 6224
[12] Bertram M, Beta C, Rotermund H H and Ertl G 2003 Complex patterns in a periodically forced surface reaction *J. Phys. Chem.* B **107** 9610–5
[13] Beta C 2004 Controlling chemical turbulence in surface reactions *Dissertation* Freie Universität Berlin, Berlin
[14] Beta C, Moula M G, Rotermund H H and Ertl G 2004 Excitable CO oxidation on Pt(110) under nonuniform coupling *Phys. Rev. Lett.* **93** 188302–6
[15] Wolff J, Papathanasiou A G, Kevrekidis I G, Rotermund H H and Ertl G 2001 Spatiotemporal addressing of surface activity *Science* **294** 134–7
[16] Qiao L, Kevrekidis I G, Punckt C and Rotermund H H 2006 Guiding chemical pulses through geometry: Y junctions *Science* **73** 6219
[17] Eiswirth M and Ertl G 1988 Forced-oscillations of a self-oscillating surface-reaction *Phys. Rev. Lett.* **60** 1526–9
[18] Rotermund H H, Engel W, Kordesch M and Ertl G 1990 Imaging of spatiotemporal pattern evolution during carbon-monoxide oxidation on platinum *Nature* **343** 355–7
[19] Gambaudo J M 1985 Perturbation of a Hopf-bifurcation by an external time-periodic forcing *J. Diff. Eqns* **57** 172–99
[20] Coullet P, Lega J, Houchmanzadeh B and Lajzerowicz J 1990 Breaking chirality in nonequilibrium systems *Phy. Rev. Lett.* **65** 1352–5
[21] Coullet P and Emilsson K 1992 Pattern-formation in the strong resonant forcing of spatially distributed oscillators *Physica* A **188** 190–200
[22] Elphick C, Hagberg A and Meron E 1998 Phase front instability in periodically forced oscillatory systems *Phy. Rev. Lett.* **80** 5007–10
[23] Hemming C and Kapral R 2001 Turbulent fronts in resonantly forced oscillatory systems *Faraday Discuss.* **120** 371–82
[24] Yochelis A 2002 Development of standing-wave labyrinthine patterns *J. Appl. Dynamical Syst.* **1** 236–47
[25] Park H K 2001 Frequency locking in spatially extended systems *Phys. Rev. Lett.* **86** 1130–3
[26] Chate H, Pikovsky A and Rudzick O 1999 Forcing oscillatory media: phase kinks vs. synchronization *Physica* D **131** 17–30
[27] Kim J, Lee J and Kahng B 1999 Harmonic forcing of an extended oscillatory system: homogeneous and periodic solutions *Phys. Rev.* E **72** 6208
[28] Davidsen J, Mikhailov A and Kapral R 2005 Front explosion in a periodically forced surface reaction *Phys. Rev.* E **72** 6214
[29] Krischer K, Eiswirth M and Ertl G 1992 Oscillatory CO oxidation on Pt(110)—modeling of temporal self-organization *J. Chem. Phys.* **96** 9161–72
[30] Hemming C and Kapral R 2002 Front explosion in a resonantly forced complex Ginzburg–Landau system *J. Chem. Phys.* D **168** 10–22

[31] Hemming C and Kapral R 2002 Phase front dynamics in inhomogeneously forced oscillatory systems *Physica* A **306** 199–210
[32] Dushman S 1949 *Scientific Foundations of Vacuum Technique* (New York: Wiley)
[33] Beta C, Mikhailov A S, Rotermund H H and Ertl G 2006 Defect-mediated turbulence in a catalytic surface reaction *Europhys. Lett.* **75** 868–74
[34] Ladas S, Imbihl R and Ertl G 1988 Kinetic oscillations and facetting during the catalytic CO oxidation on Pt(110) *Surf. Sci.* **198** 42–68
[35] Mikhailov A S and Showalter K 2006 Control of waves, patterns and turbulence in chemical systems *Phys. Rep.* **425** 79–194